A&A 473, 239–243 (2007)
DOI: 10.1051/0004-6361:20077802

Astronomy & Astrophysics

Spectroscopic evidence of velocity fields at the surface of ZZ Ceti stars

D. Koester and E. Kompa

Institut für Theoretische Physik und Astrophysik, University of Kiel, 24098 Kiel, Germany
e-mail: koester@astrophysik.uni-kiel.de

Received 7 May 2007 / Accepted 8 July 2007

ABSTRACT

Aims. High resolution spectra of DA and DAZ white dwarfs show peculiar line profiles for objects in or near the ZZ Ceti instability strip. The lines are broader and shallower than in slightly hotter or cooler objects. Rotational broadening could produce a similar effect but several of the objects are known to be very slow rotators. We therefore study here whether these profiles could be caused by velocity fields on the surface originating from the pulsation of the stars.
Methods. Theoretical line profiles are simulated by dividing the projected stellar disk into many small area elements. The intensity at each point in the direction of the observer is calculated from accurate theoretical atmosphere models, and the contributions are summed up, taking into account Doppler shifts from the velocity field.
Results. We obtain predicted light curves, variation of the average line-of-sight velocity, of the distribution of radial velocity over the visible surface, and of spectral line profiles for the Ca II K resonance line.
Conclusions. The predicted line profiles are very similar to those observed. It is thus very plausible that indeed the pulsations and associated velocity fields are at the origin of these peculiarities.

Key words. stars: white dwarfs – stars: oscillations

1. Introduction

During the spectroscopic search for rotation in hydrogen atmosphere (DA) white dwarfs Koester et al. (1998) noticed peculiar Hα line profiles in four objects. In contrast to most of the DA white dwarfs, where the narrow NLTE-cores of Hα can be fit very well with a theoretical profile of a non-rotating star, these objects showed a much flatter core. Three of the four stars were known to be pulsating ZZ Ceti stars, the fourth (WD 1544-377) has an effective temperature close to the instability strip. Fitting the lines with rotationally broadened profiles resulted formally in projected rotational velocities of $v \sin i \approx 40$–$50\,\mathrm{km\,s^{-1}}$, but poor fits. While it seemed highly unlikely that a cooling DA could suddenly acquire a large angular momentum when reaching the instability strip, such large rotation velocities were also excluded in the case of the three ZZ Cetis from asteroseismology measurements of the pulsational frequency splittings (see Koester et al. 1998, for a discussion).

An obvious alternative explanation for the line profiles were surface motions associated with the non-radial pulsations. Such motions were indeed discovered in ZZ Cetis by van Kerkwijk et al. (2000); Thompson et al. (2003); Kotak et al. (2002) and by Kotak et al. (2003) in a variable DB. Thompson et al. (2003) concluded that the observed pulsational line shifts could not explain the flat core profiles; their test, however, considered only shifts and not any intrinsic broadening due to a distribution of velocities over the surface at any point in time, and may thus not be conclusive.

The next step was reached in the study of rotational velocities by Berger et al. (2005) using the extremely narrow and sharp Ca II K resonance line in DAZs with high-resolution spectra from the Keck telescope and the ESO VLT. In seven high signal-to-noise spectra of the well known variable G 29-38 the lines showed much smaller central depth than in a theoretical non-rotating star, with apparent "rotational velocities" from 10.7 to $28.0\,\mathrm{km\,s^{-1}}$ over a period of a few years. Since it is impossible for a white dwarf to change the rotation on such a timescale, rotation was definitely ruled out as the cause of the peculiar profiles. On the basis of similar profiles the authors predicted variability for WD 1150-153, which was confirmed independently by Voss et al. (2007) and Gianninas et al. (2006).

The narrow Ca lines offered the possibility to study rotation spectroscopically with higher accuracy than from the Hα line. It is also well suited for a study of other surface velocity fields, such as might arise from pulsation. In this paper we are trying such an approach with the calculation of realistic line profiles by direct numerical integration over the visible surface of the star, including velocities as predicted by pulsation theory, accurate theoretical spectra for the intensity as function of wavelength and angle against surface normal (i.e. limb darkening), and the geometry and Doppler shifts in the observers frame.

2. Modeling the observable line profiles

The variation of the energy flux ΔF at the surface of a non-radially pulsating white dwarf can be written as (Dziembowski 1977)

$$\Delta F = A_F\, F P_l^m(\cos\vartheta)\, \cos(\omega t + m\varphi + \varphi_0) \qquad (1)$$

with the amplitude A_F, polar coordinates ϑ, φ, angular frequency ω, time t, and a possible phase shift φ_0. The "quantum numbers" m, l of the associated Legendre polynomial P_l^m define the mode of the oscillation.

From the theoretically predicted local flux F we determine a local effective temperature, using the relation $F = \sigma {T_{\rm eff}}^4$. This temperature is then used to interpolate within a grid of model atmospheres to obtain the intensity at this point of the surface as a function of wavelength and θ, the angle against the normal on the stellar surface $I(T_{\rm eff}, \lambda, \theta)$. The surface gravity is held constant during the pulsation, because the radius change is negligible (see below).

Also from Dziembowski (1977), with slight changes of notation, we obtain the three components of the velocity V at the surface of the star

$$V_r = -\frac{V_0}{a} N P_l^m(\cos\vartheta) \cos(\omega t + m\varphi) \quad (2)$$

$$V_\vartheta = -V_0 N \frac{\partial}{\partial\vartheta} P_l^m(\cos\vartheta) \cos(\omega t + m\varphi) \quad (3)$$

$$V_\varphi = -V_0 N P_l^m(\cos\vartheta) \cos(\omega t + m\varphi)/\sin\vartheta \quad (4)$$

with the radial coordinate r. Here

$$a = \frac{GM}{\omega^2 R^3} \quad (5)$$

(G gravitational constant, M, R mass and radius of the star), which is approximately the square of the ratio of the pulsation period to the dynamical time scale. For a non-radially pulsating white dwarf this is a large number and radial motions are therefore completely negligible (Dziembowski 1977; Robinson et al. 1982). N is a normalization constant, which we have fixed in such a way that the maximum value of any angular component on the surface is V_0. This value thus sets the amplitude of the velocity variations, as does A_F for the flux variations. These values describe the maximum intrinsic amplitudes on the stellar surface and should not be confused with the observed amplitudes, which are always smaller due to the averaging over the stellar disk (see below).

The spectrum measured by a distant observer is given by the integration over the visible disk of the intensity along the line-of-sight, Doppler shifted according to the velocity component pointing towards the observer v, and divided by the disk area. The appropriate coordinate system for the stellar disk is a two-dimensional polar system with distance from the center of the disk ρ (in units of the disk radius) and angular coordinate ϕ.

$$\bar{I} = \frac{1}{\pi} \int_0^{2\pi} \int_0^1 I(T_{\rm eff}, \lambda(1 + v/c), \theta)\, \rho \mathrm{d}\rho\, \mathrm{d}\phi \quad (6)$$

with the geometric relation $\sin\theta = \rho$. The local effective temperature and the line-of-sight velocity v will usually depend on ρ and ϕ.

The transformation between the two reference frames (star and observer) is facilitated significantly with the introduction of two intermediate Cartesian coordinate systems. The first rotation around the line-of-sight matches the projection of the stellar pulsation axis on the sky, the second around an intermediate axis aligns the original line-of-sight with the axis. These rotations are described by two simple rotation matrices.The only physically meaningful rotation for spatially unresolved observations is of course the angle between line-of-sight and stellar pulsation axis.

The integration over the visible disk is carried out numerically by dividing the disk into a large number of small area elements, using approximately 100 intervals for the radius and 360–720 for the angular integration. The intensities at each point into the direction of the observer are calculated from the local effective temperature and the model atmosphere grid. They are weighted with the relative size of the element, the wavelengths are shifted according to the local line-of-sight velocity and then summed up to give the disk-averaged intensity. This is of course – after multiplication with the solid angle of the star – the observable spectral energy flux. Repeating this for several time steps throughout the period of an oscillation results in theoretical time-resolved spectra, light curves, line profiles, and equivalent widths. In order to help with the interpretation of the numerical results we define and calculate two further quantities

$$\bar{v} = \frac{1}{\pi\bar{I}} \int_0^{2\pi} \int_0^1 v\, I(T_{\rm eff}, \lambda(1 + v/c), \theta)\, \rho \mathrm{d}\rho\, \mathrm{d}\phi \quad (7)$$

which is a weighted average radial velocity, and

$$\sigma^2 = \frac{1}{\pi\bar{I}} \int_0^{2\pi} \int_0^1 v^2\, I(T_{\rm eff}, \lambda(1 + v/c), \theta)\, \rho \mathrm{d}\rho\, \mathrm{d}\phi - \bar{v}^2 \quad (8)$$

which characterizes the distribution of radial velocities over the disk. Obviously, $\bar{v}$ is responsible for any shift of a spectral line, and σ for a "pulsational broadening", analogous to the "rotational broadening" in a rotating star.

Table 1. Seven high-resolution spectra used for the comparison with our theoretical line profile and equivalent width calculations. The spectral resolution is 34 000 at the Keck and 18 500 at the VLT. Given are the Julian Date of the observation, the exposure time, and the equivalent width of the Ca II K line.

Spectrum	MJD – 2 400 000	Exp [s]	EW [Å]	Source
S1	51 762.680802	300	0.237	ESO/VLT
S2	51 804.670030	300	0.244	ESO/VLT
K1	51 158.178672	1800	0.246	Keck
K2	50 636.556137	1800	0.243	Keck
K3	51 403.464512	1800	0.264	Keck
K4	51 403.442454	1800	0.260	Keck
K5	51 403.413265	1800	0.261	Keck

3. Observational data

This is a pilot study of a possible explanation for the peculiar line profiles in ZZ Ceti stars. Although we do not aim at a detailed fit of observed data, the feasibility of this explanation can only be demonstrated with a comparison with real, observed profiles. For this purpose we use seven high-resolution spectra of the bright ZZ Ceti star G 29-38 (=WD 2326+029). These spectra were originally taken for different programs: the search for metals in DA white dwarfs at the Keck telescope (Zuckerman et al. 2003), and the ESO Supernova Ia Progenitor Survey (Napiwotzki et al. 2001). More information about the observations and reductions can be found in those papers and in Koester et al. (2001, 2005); Berger et al. (2005).

4. Results

Our first exploratory calculations used the following parameters: the atmospheric model for the non-pulsating star was a DAZ, hydrogen-dominated atmosphere with traces of calcium, $T_{\rm eff}$ = 11 600 K, $\log g = 8.0$, Ca/H ratio 4.5×10^{-7} by numbers. These values are close to the data for G 29-38, our test case (Berger et al. 2005).

Thompson et al. (2003) list the observed oscillation modes for G 29-38. The dominant periods are in the range 400–800 s, the largest flux amplitude 2.88%, and the largest velocity amplitude 4.53 km s^{-1}. The observations were obtained in the optical range, and the flux amplitudes refer to the visual magnitude V, not the total luminosity. Our model spectra were only calculated for an interval around the Ca II line, but since the amplitudes do not change greatly through the optical range, we have used our predicted continuum flux at 3930 Å as the closest approximation to the observations. This could be improved by extending the theoretical calculations to longer wavelengths, but in view of the exploratory nature of this study we did not consider this necessary.

One should note that the observed amplitudes are averages over the visible stellar disk. Depending on the oscillation mode as described by l, m, one or more node lines will cross the disk, separating e.g. areas brighter than average from fainter ones. On the node lines the amplitudes are by definition zero, and over most of the surface they take values between the maximum and zero. The maximum intrinsic values A_F and V_0, as defined in our Eqs. (1)–(4), which are the absolute maxima over the stellar surface, will thus never be observable. In order to obtain numbers in our final calculations (see below) comparable to the observed amplitudes, which are significantly decreased by these cancellation effects, our initial test used a single mode with $l = 1, m = 0$, pole-on view of the star, period 600 s, $V_0 = 20$ km s^{-1}, $A_F = 12\%$, phase shift between flux and velocity variation 50°.

Figure 1 shows the simulated light curve over one period (top panel). The observable amplitude is about 1/2 of the intrinsic amplitude in the star, due to cancellation and limb-darkening effects. The disk-averaged radial velocity (observable line-of-sight radial velocity (middle panel) is also reduced by a factor of 2 compared to V_0. This velocity component will lead to a systematic shift of a spectral line.

Both amplitudes, for the flux and the radial velocity, are still about a factor of 2–3 larger than observed for any *single* mode. We believe that these higher values are realistic, if we try to represent G 29-38, which has at least seven modes of comparable strength, with one single mode. We will come back to this issue below. The distribution of line-of-sight velocities over the visible surface, as defined in Eq. (8), is displayed in the bottom panel of Fig. 1. Through the Doppler effect this will lead to significant and highly variable broadening of narrow spectral lines. Both of these effects, line shift and broadening, are clearly demonstrated in Fig. 2, which compares the theoretical profile of our pulsating model at four different phases with the profile of a non-pulsating model and with an observed spectrum of G 29-38 from the Keck telescope. The observed spectrum is integrated over 1800 s, i.e. over several periods of all known modes. As could be expected from Fig.1, the pulsation effect almost disappears at phases 0.0 and 0.5, and is strongest at 0.25 and 0.75.

As these white dwarfs are rather faint, observed spectra intended to determine spectral types or stellar parameters – in particular when using higher spectral resolution – will use long exposure times, typically 30 to 60 min. These are longer than the pulsation periods. In Fig. 3 we compare three long Keck exposures (1800 s) with the theoretical line profile of our model, integrated over one period. The spectrum with the deepest line is reproduced perfectly; the other spectra seem to require still larger pulsation amplitudes.

For a final, more realistic test we have used the seven modes found by Thompson et al. (2003) and described in their Table 1. We take directly their periods and phase shifts, but have

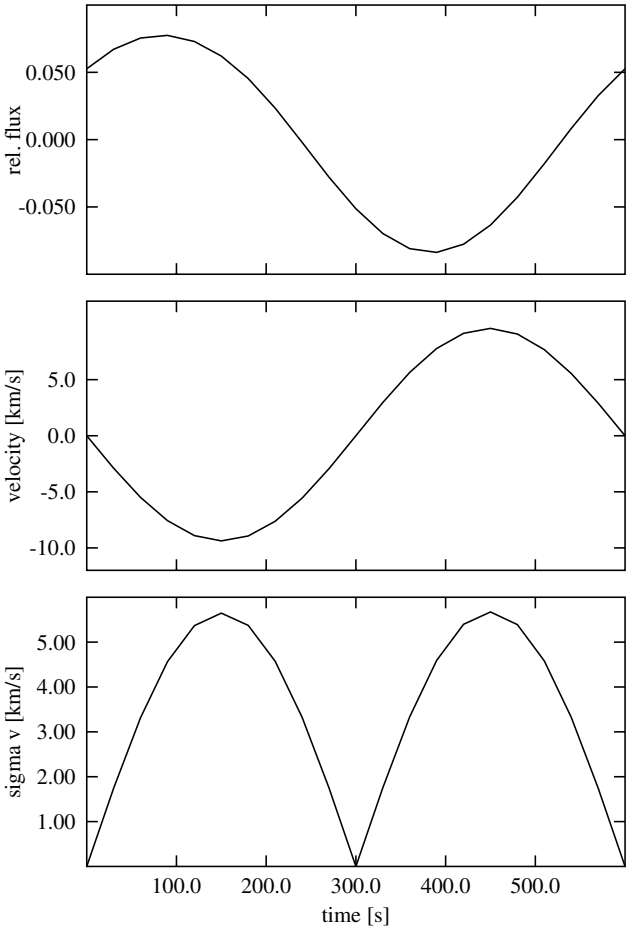

Fig. 1. *Top panel*: simulated theoretical light curve (continuum at 3930 Å) for a single mode oscillation as described in the text. *Middle*: simulated disk-averaged line-of-sight velocity for the same oscillation. *Bottom*: simulated distribution of the line-of-sight velocity component over the stellar surface σ, as defined in Eq. (8).

increased their amplitudes by a factor of two to account for the intrinsic amplitude variation on the surface and cancellation effects. As described for the simpler example above, the spectra at each point of the visible surface are Doppler shifted and corrected for the limb darkening, before integrating over the surface. The resulting intensity and radial velocity curves are displayed in Fig. 4. These theoretical curves show very good qualitative agreement with the observed curves in Fig. 4 of Thompson et al. (2003). This agreement is of course not totally unexpected, since the periods and amplitudes were determined from a Fourier analysis of the observed light curves. Nevertheless, the agreement is a test for our numerical integration procedures and, even more important, for the scaling we apply to determine the intrinsic amplitudes A_F and V_0. Taking 300 s integrations over different intervals in the light curves, with large and small variations, we find line profiles similar to those in Figs. 1 and 2, and equivalent widths varying by about 10%. This is in good agreement with the observed values in Table 1. A close comparison of our simulation with the observations shows that our predicted amplitudes are still somewhat smaller thanobserved. This is in line with the finding (Fig. 3) that our predicted profile is still too deep compared to some observed spectra. The solution would be to increase the factor we have used for the cancellation effect from 2 to perhaps 2.3–2.5.

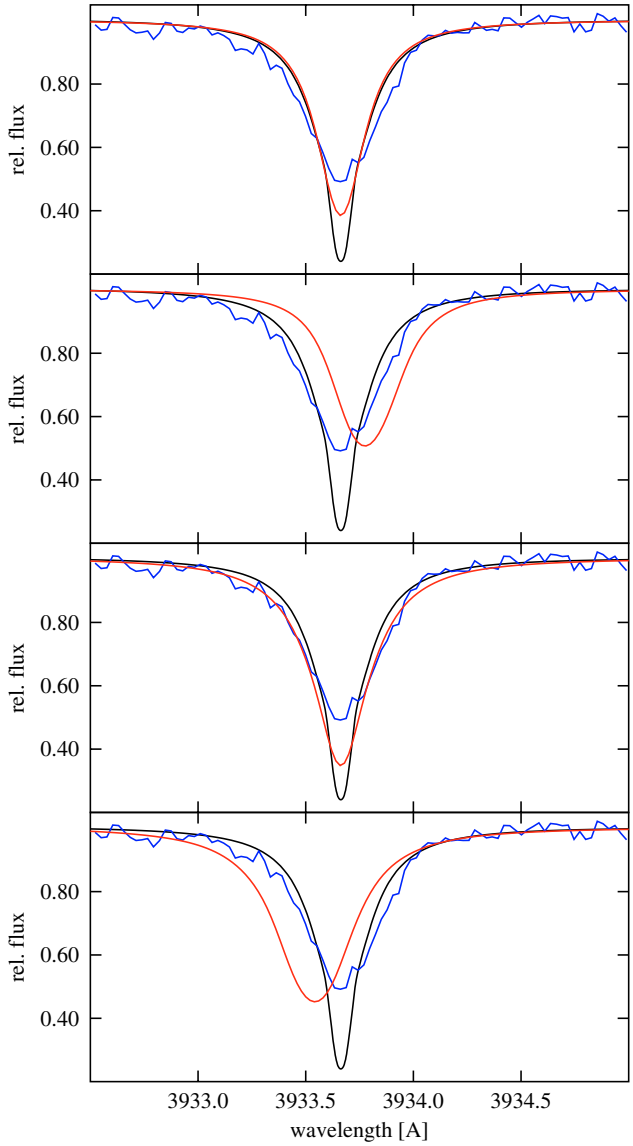

Fig. 2. Variation of the CaII K line profile over one period. *From top to bottom* are the pulsation phases 0.0, 0.25, 0.5, 0.75. The deepest line (black, the same in all panels) is the theoretical profile of a non-pulsating star. The noisy (blue) line is an observed line in one of the Keck spectra, integrated over several periods (1800s). This line is also the same in all panels. The third (red) line is the theoretical profile of a white dwarf pulsating in the $l = 1$, $m = 0$ mode at 4 different phase in the cycle.

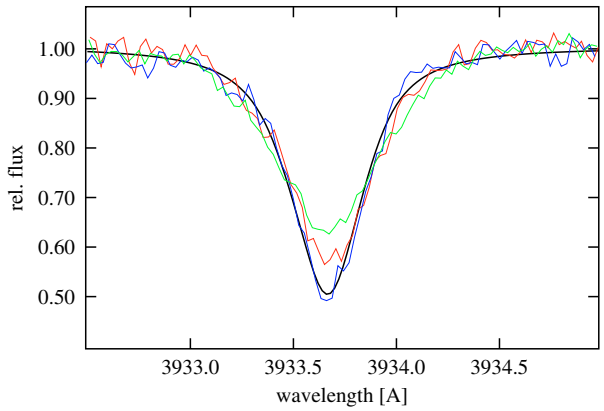

Fig. 3. Time integrated theoretical line profile (thick black) compared with three different Keck spectra (thin, colored lines).

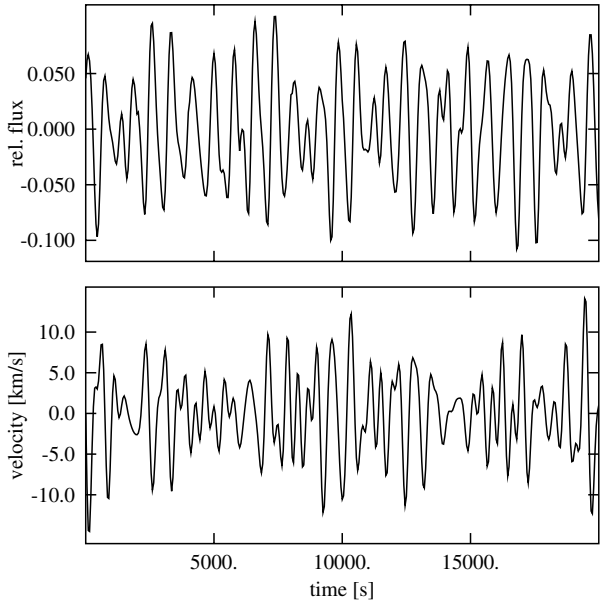

Fig. 4. Simulated light and radial velocity curves using the seven oscillation modes identified in Thompson et al. (2003).

In a recent paper von Hippel & Thompson (2007) found a change in equivalent of almost a factor of 2 over a period of 5 years. Their most extreme values were taken from very different observations (time resolved spectra with very short integration times), and may not be totally comparable to the more direct observations presented in our Table 1. However, if such variations are confirmed, our calculations show that they are very likely not due to the pulsations, but could indicate a change in accretion rates.

5. Conclusions

Our observational data consist of several high resolution, high S/N spectra of the Ca II K resonance line in G 29-38, and a set of pulsation periods, modes, and light and velocity amplitudes from the literature. Both sets of data were obtained at different times, with different projects in mind. Mainly for this reason we have in this study not attempted to achieve a real fit to light curves or spectral line profiles. We have shown that it is quite possible that the peculiar Hα and Ca II line profiles observed in some DA and DAZ white dwarfs in or near the ZZ Ceti instability strip are in fact caused by surface motions due to the non-radial pulsations. At any point in time different parts of the visible surface may move with different velocities along the line-of-sight of the observer, leading to a broadening of spectral lines analogous to rotational broadening. In addition, for longer exposure times of a significant fraction of the major periods, the systematic shift caused by the variation of the average radial velocity leads to a further increase of the broadening. Both effects combined lead to spectral line shapes in our simulations, which are quite similar to those observed.

The emphasis in this exploratory study was on understanding the peculiar line profiles, which have been a puzzle since

ten years. It particular it should be very clear now that rotation does not have to be invoked as an explanation, which of course was always regarded as extremely unlikely. In a future study we will apply the methods developed here for the more general calculation of time-dependent spectra of variable white dwarfs. This has over the past years become a supplementary method to standard asteroseismology for the determination of pulsation modes and stellar parameters. There are some remaining discrepancies between simulations and observed wavelength dependent amplitudes in the Balmer line cores, which we believe may be caused by the current neglect of the velocity fields.

References

Berger, L., Koester, D., Napiwotzki, R., Reid, I. N., & Zuckerman, B. 2005, A&A, 444, 565
Dziembowski, W. 1977, Acta Astron., 27, 95
Gianninas, A., Bergeron, P., & Fontaine, G. 2006, AJ, 132, 831
Koester, D., Dreizler, S., Weidemann, V., & Allard, N. F. 1998, A&A, 338, 612
Koester, D., Napiwotzki, R., Christlieb, N., et al. 2001, A&A, 378, 556
Koester, D., Rollenhagen, K., Napiwotzki, R., et al. 2005, in 14th European Workshop on White Dwarfs, ed. D. Koester & S. Moehler, ASP Conf. Ser., 334, 215
Kotak, R., van Kerkwijk, M. H., Clemens, J. C., & Bida, T. A. 2002, A&A, 391, 1005
Kotak, R., van Kerkwijk, M. H., Clemens, J. C., & Koester, D. 2003, A&A, 397, 1043
Napiwotzki, R., Christlieb, N., Drechsel, H., et al. 2001, Astron. Nachr., 322, 411
Robinson, E. L., Kepler, S. O., & Nather, R. E. 1982, ApJ, 259, 219
Thompson, S. E., Clemens, J. C., van Kerkwijk, M. H., & Koester, D. 2003, ApJ, 589, 921
van Kerkwijk, M. H., Clemens, J. C., & Wu, Y. 2000, MNRAS, 314, 209
von Hippel, T., & Thompson, S. E. 2007 [arXive:astro-ph/0702663]
Voss, B., Koester, D., Østensen, R., et al. 2007 [arXiv:astro-ph/07042710]
Zuckerman, B., Koester, D., Reid, I. N., & Hünsch, M. 2003, ApJ, 596, 477